Biointerface Research in Applied Chemistry
Open-Access Journal (ISSN: 2069-5837)

Article
Volume 15, Issue 2, 2025, 26
https://doi.org/10.33263/BRIAC152.026

Effect of Dinitrosyl-Iron Complexes (Nitric Oxide Donors) on Cell Morphology and Nuclear Structure

Natalia Akentieva [1,*], Natalia Sanina [1,2], Kseniya Popovicheva [2], Artur Gizatullin [1], Stanislav Shram [3], Sain Shushanov [4]

[1] Laboratory Biochemical and Cellular Studies, Department Kinetics of Chemical and Biological Processes, Federal Research Center of Problems of Chemical Physics and Medicinal Chemistry Russian Academy of Sciences, Academician Semenov avenue 1, City Chernogolovka, Moscow Region 142432, Russia; na_aken@icp.ac.ru;
[2] Lomonosov Moscow State University, Kolmogorova avenue 1, City Moscow 119991, Russia; sanina@icp.ac.ru (N.S.); ksen.4bramova@yandex.ru (K.P.);
[3] Laboratory of Molecular Pharmacology of Peptides, Department of Molecular Immunology and Pharmacology, National Research Centre «Kurchatov Institute», Kurchatov Sq. 2, Moscow 123182, Russia; shram.img@yandex.ru (S.S.);
[4] Laboratory genetics of cancer cells, FSBI «N.N. Blokhin NMRCO» of the Ministry of Health of the Russian Federation, st. Kashirskoe Highway 24, City Moscow 123182, Russia; sainhershy@yandex.com (S.S.);
* Correspondence: na_aken@icp.ac.ru (N.A.);

Scopus Author ID56370037400
Received: 26.09.2024; Accepted: 2.01.2025; Published: 15.04.2025

Abstract: Dinitrosyl iron complexes (nitric oxide donors) can be used in cardiology for the treatment of cardiovascular diseases and in oncology as an antitumor drug. Therefore, synthesizing new dinitrosyl iron complexes (DNICs) and studying the mechanism of their action is a relevant and important task. The effect of dinitrosyl iron complexes (cytoprotector and cytostatic) on the morphology and nuclear structure of cells was studied using confocal fluorescence microscopy. The results showed that when human lung fibroblasts were treated with a low concentration of DNIC#4 (cytoprotector), the cell morphology and nuclear structure remained virtually unchanged; the actin structure consisted of long, well-organized fibers and the nuclei had a rounded shape. It was found that after treating multiple myeloma cells with DNIC#7 (cytostatic), dramatic changes in cell morphology were observed, actin fibers and cytoplasmic membranes were destroyed, and the nuclei were fragmented. Thus, the results confirm that DNIC#4 exhibits a cytoprotective effect on cells at low concentrations, and DNIC#7 is a cytotoxic compound. Therefore, DNIC#4 has potential for use in cardiology, and DNIC#7 has potential for the treatment of human multiple myeloma.

Keywords: dinitrosyl iron complexes; multiple myeloma; cell morphology; nuclear structure; fibroblasts.

1. Introduction

Mortality from cardiovascular diseases (CVD) ranks first in all countries [1, 2]. Cardiovascular diseases account for 49% of the causes of all deaths in Europe [3]. Disability and mortality from cardiovascular diseases are major problems in many countries, and the costs of treating CVDs have increased significantly in low- and middle-income countries. [4]. Currently, available antihypertensive drugs are characterized by short-term effects and exhibit many side effects, such as hypokalemia, cardiovascular complications, and so on [5-7]. In this regard, searching for and synthesizing new cardiac drugs, studying their properties and characteristics, and their effect on the body's cells is an important task.

The key role of nitric oxide (NO) in regulating vascular tone and myocardial metabolism has been established. [8, 9]. Nitric oxide has been shown to be a signaling molecule that regulates many metabolic and pathological processes in the human body. [10-12]. Nitric oxide exhibits a protective effect against the development and progression of cardiovascular diseases; this molecule affects the contraction of blood vessels, relaxes smooth muscles, exhibits anti-coagulant properties, inhibits monocyte adhesion, low-density lipoprotein oxidation, and cytokine synthesis, as well as influences the immune response and neurotransmission [13-18].

NO concentration is a key factor determining its biological effects [19, 20]. It is known that at high concentrations (> 1 μM), NO is cytotoxic because it forms a toxic compound called peroxynitrite [21]. At the same time, it has been shown that low concentrations of NO (<1 μM) exhibit cytoprotective properties and have a positive effect on the homeostasis of the cardiovascular and nervous systems[22, 23].

Currently, in medical practice, for the treatment of the cardiovascular system, the use of drugs based on nitric oxide donors is relevant [24,25]. NO donors are dinitrosyl iron complexes (DNICs), which are currently widely used in practice. Many of their functions have been discovered over the entire period of studying DNICs, ranging from vasodilator and hypotensive to antitumor activity [26,27]. It is known that DNICs have a positive effect on many processes inside the body. Namely, they relax blood vessels, lower blood pressure, and prevent the formation of blood clots [28-30]. The ability to neutralize secondary lipid peroxidation products allows them to exhibit antioxidant properties [31]. It is known that DNICs increase erythrocytes' elasticity, accelerate wound healing, and inhibit platelet fusion and apoptosis of normal body cells [32-34]. Excess NO also has biological effects, the meaning of which is to inactivate iron-containing enzymes and inhibit cell growth and development [35,36].

Along with regulating tumor growth by nitric oxide, DNICs also trigger the process of suppressing tumor growth [37,38]. This is due to the rapid destruction of DNICs in actively dividing cells and the release of large amounts of NO. It is known that in high concentrations, NO is an activator of apoptosis [39]. It is known from the literature that in human leukemia cells, NO triggers apoptosis through the activation of caspases [40,41].

It should be noted that cationic DNICs with sulfur-containing ligands—thiourea and its derivatives—were synthesized by us earlier. [42,43]. We have shown that DNICs are effective inhibitors of enzymes that are biomarkers of CVD: myeloperoxidase, renin, matrix metalloproteinase, and poly(ADP-ribose)polymerase [44-50]. Previous studies have shown that DNIC#4 exhibits cytoprotective properties [44-48,50], while DNIC#7 is cytostatic and exhibits toxicity to multiple myeloma cells [46,49].

However, there is no information in the literature on the effect of these compounds on the morphology and nuclear structure of the cell. Therefore, this study aimed to conduct a comparative analysis of the effect of DNIC#4 (cytoprotector) and DNIC#7 (cytostatic) on the morphology and structure of the cell nucleus.

2. Materials and Methods

2.1. Materials.

The growth medium DMEM (low glucose-1 g/l, L-glutamine, 25 mM HEPES, sodium pyruvate, Biowest, France), gentamicin (10 mg/ml, Biowest, France), HyClone Fetal Clone III

Serum (GE Healthcare, USA), was used in this work. The growth medium RPMI-1640, modified to contain 2 mM L-glutamine, 10 mM HEPES, 1 mM sodium pyruvate, 4500 mg/L glucose, and 1500 mg/L sodium bicarbonate, was used in this work (OOO NPP PanEco, Russia). FITC-phalloidin (Enzo Life Sciences, USA) and Hoechst 33258 (Sigma, Germany) were used to stain cells. A mounting (Fluoro Gel-11) medium was used in this work (Electron Microscopy Sciences, USA). Plastic dishes (25 cm culture bottles, disposable pipettes) for growing cell cultures were purchased from Corning-Costar (USA).

2.2. Cell lines.

The work used human multiple myeloma cells (MM, cell line RPMI 8226, kindly provided by S.S. Shushanov, N.N. Blokhin National Medical Research Center of Oncology, Ministry of Health of Russia, Moscow). Origin of the indicated cell line: human, bone marrow, myeloma. Adhesive Human lung-derived embryonic fibroblasts (line *FLEH-104*) were purchased from the Russian Collection of Vertebrate Cell Cultures (BioloT, St. Petersburg, Russia).

2.3. Cultivation of a human multiple myeloma cell line.

Culture method: cells were grown in suspension in RPMI medium with 10% fetal calf serum at 37°C, 5% CO_2, and 95% humidity. Cells were grown to 90% density in culture flasks and then used for experiments.

2.4. Cultivation of a cell line of fibroblast lung embryo cells

Fibroblast lung embryo cells (*FLEH-104)* were cultured in DMEM growth medium supplemented with 10% (vol/vol) fetal bovine serum solution and 10 mM HEPES at pH 7.2. The cell culture was incubated in a humidified atmosphere (90%), 5% CO_2 at 37^0. After reaching 90% cell density, the cells were treated with a solution of 0.25% trypsin-EDTA, centrifuged at 3000 g for 5 min, the supernatant fraction was discarded, and the cells were resuspended in growth medium and seeded on glass substrates in wells in a 24-well plate.

2.5. Synthesis of the dinitrosyl iron complexes.

To study dinitrosyl iron complexes (DNICs) on cell morphology and nucleus, we used mononuclear dinitrosyl iron complexes with functional sulfur-containing ligands, namely thiourea and its derivatives: $[Fe(SC(NH_2)(NHC_2H_5))_2(NO)_2]Cl$[$Fe(SC(NH_2)(NHC_2H_5))Cl(NO)_2]$ (#4) and $[Fe(SC(NHCH_3)_2)_2(NO)_2]BF_4$ (#7). The compounds were synthesized according to the protocol [42, 43]. The molecular structure of DNIC#4 and DNIC#7 was confirmed by X-ray diffraction, Mössbauer, IR, and EPR spectroscopy [51-57]. It was established that when dissolved in aqueous solvents, DNIC#4 and DNIC#7 release NO as a result of complex dissociation [58].

2.6. Effect of DNIC#4 on the morphology and chromatin structure of FLEH.

Cells *FLEH-104* were seeded onto glass substrates into wells in a 24-well plate and grown for 24 hours. The old growth medium was removed by aspiration, and a new one was added, adding various concentrations of DNIC#4. In particular, 100 µl of DNIC#4 [$4x10^{-3}$M] (3 wells) was added to 900 µl of DMEM growth medium, and also to 990 µl of growth medium

was added to 10 µl of DNIC#4 [4x10^{-4}M] (3 wells), only growth medium was added to control wells (3 wells). Then, the plate with cells was incubated at 37º in an atmosphere of 5% CO_2 and 95% humidity for 24 hours.

2.7. Effect of DNIC#7 on the morphology and chromatin structure of multiple myeloma cells.

MM cells were seeded in two culture flasks and grown for 8 days; fresh growth medium was added every 3-4 days. After 8 days, DNIC#7 (3.4 x 10^{-3}M) was added to the experimental flask, and only growth medium was added to the control flask. The vials were then incubated at 37º in an atmosphere of 5% CO_2 and 95% humidity for 24 hours.

2.8. Fixation and staining of cells with fluorescent dyes.

After 24-hour incubation with DNICs, cell samples (*FLEH* и MM) were fixed for 10 min at room temperature with 2.0% formaldehyde and 5% glucose in PBS, 0.1 M, pH = 7.2 (500 µl/well). Then, the fixing solution was removed and washed 2 times with PBS buffer (500 µl/well). After this, 500 µl of blocking solution (bovine albumin + Triton X-100 in PBS) was added to the wells and incubated for 30 min at 37º. The blocking solution was then removed with a micropipette, and the cells were washed twice with PBS. After this step, 200 µl of PBS and 10 µl of FITC-phalloidin solution (2 µg/ml) were added to each well and incubated for 1 hour at room temperature. FITC-phalloidin was then removed, and the cells were again washed 3 times with PBS (500 µl/well). After this, 1 ml of PBS and 10 µl of Hoechst 33342 solution (final concentration 0.2 µg/ml) were added to each well and incubated for 30 min at a temperature 37º in an atmosphere of 5% CO_2. Then, it was washed 1 time with PBS. After staining, coverslips were removed from the wells, placed on filter paper, and then covered with mounting (Fluoro Gel-11) medium. Coverslips were placed on glass slides with the side on which the *FLEH* cells were located. Since MM cells are suspended, they were placed on glass slides after fixation and staining, mounting (Fluoro Gel-11) medium was added, and coverslips were covered on top. Then, the slides were kept for 24 hours at 40°C in the dark, then the edges of the coverslip were sealed with colorless varnish. Cell and nuclear morphology were analyzed using a laser confocal microscope, as previously described [59].

2.9. Analysis of cell morphology and nuclear structure using confocal microscopy.

Microfluorescence analysis was performed on an inverted scanning confocal microscope LSM 510 META (Zeiss, Germany) using EC Plan-Neofluar 40x/1.30 Oil DIC M27 and Plan-Apochromat 63x/1.4 Oil DIC M27 objectives. Fluorescence of FITC-phalloidin and Hoechst 33342 were detected at excitation/emission wavelengths of 488/505-530 nm and 405/420-490 nm, respectively. The obtained images were processed using AxioVision 4.8 and ImageJ 1.42q software.

3. Results and Discussion

3.1. Effect of DNIC#4 (potential cytoprotector) on the morphology of FLEH cells.

The results of the study showed that in control samples (without the addition of DNIC#4), fibroblasts have normal morphology, elongated cells, and well-stained nuclei, the actin structure is visible, fibroblast filaments are elongated and clearly defined, the cytoplasmic membrane of the cells is not destroyed (Figure 1).

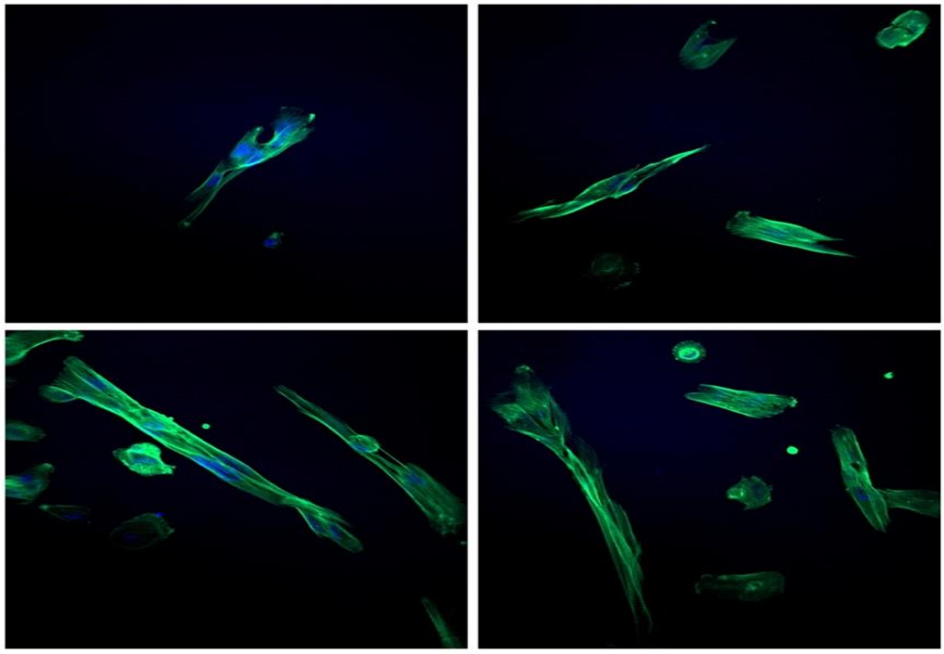

Figure 1. Confocal image of the cell morphology and nuclear structure of *FLEH* cells before treatment with DNIC#4: nuclei are shown in blue (Hoechst), while actin structure and filaments are shown in green (FITC), objective 40x. Images size – 232.5 μm x 232.5 μm.

We found that when *FLEH* cells are incubated with high concentrations of DNIC#4 [$4x10^{-3}$M], changes in cell morphology are observed. In particular, most of the cells acquire a rounded shape instead of an elongated one, the edges of the cells become uneven, the cell nuclei are poorly stained, and their structure is disturbed. The cells have practically no filaments, and actin has a loose structure. Actin fibers look destroyed, and the cytoplasmic membrane is partially destroyed (Figure 2).

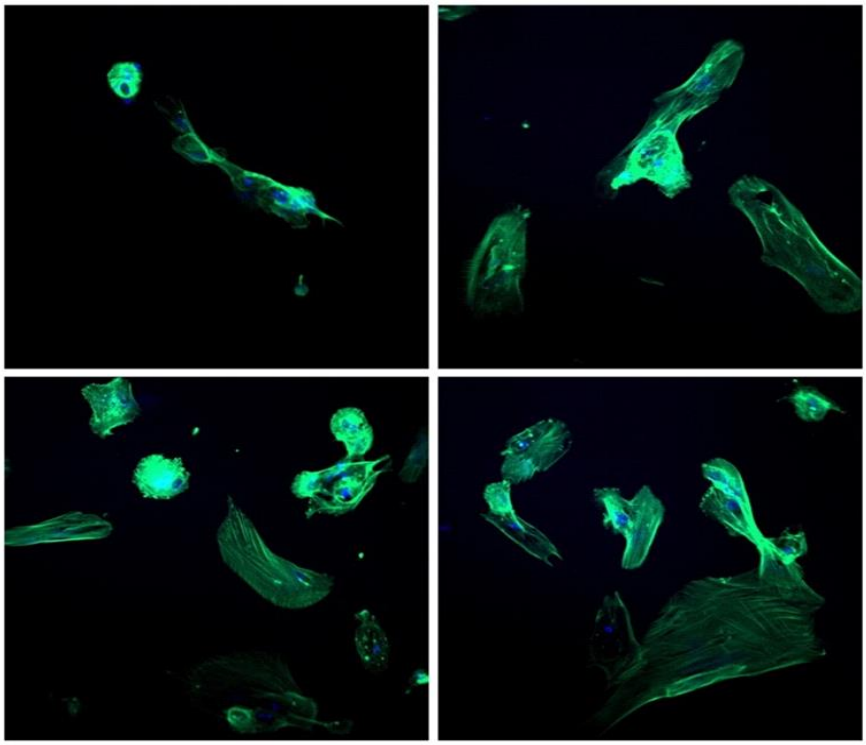

Figure 2. Confocal image of the cell morphology and nuclear structure of *FLEH* cells after treatment with DNIC#4[$4x10^{-3}$M]: nuclei are shown in blue (Hoechst), while actin structure and filaments are shown in green (FITC), objective 40x. Images size – 232.5 μm x 232.5 μm.

It is likely that the round shape of the cells is observed due to their loss of adhesiveness and the development of apoptosis. This indicates that at high concentrations of DNIC#4, significant changes in cell and nuclear morphology are observed.

However, when cells were treated with a lower concentration of DNIC4 [$4x10^{-4}$ M], it was found that the morphology of the cells practically did not change and was closer to normal control cells (without the addition of DNIC#4). Confocal images show that the shape of the cells is elongated, and colored nuclei are visible, but in smaller ones, there are filaments; however, their edges are also destructured and unclear (Figure 3).

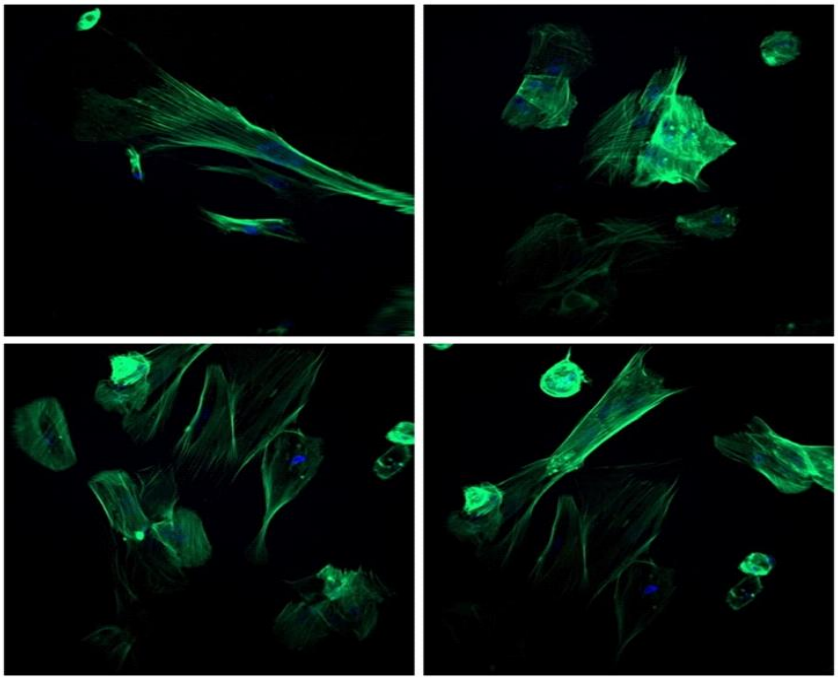

Figure 3. Cell morphology and nuclear structure of a *FLEH* cell after treatment with DNIC#4[$4x10^{-3}$M]: nuclei are shown in blue (Hoechst), actin structure and filaments are shown in green (FITC), objective 40x. Images size – 232.5 μm x 232.5 μm.

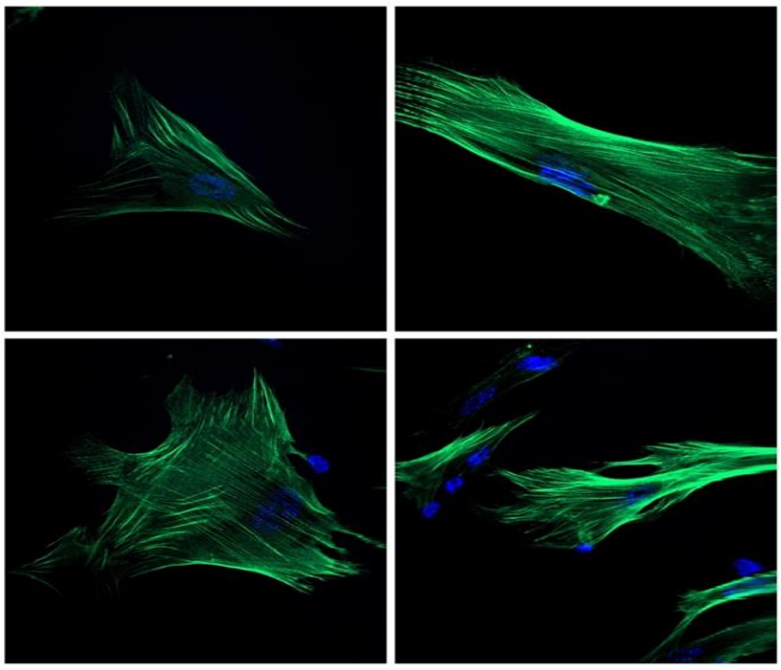

Figure 4. Cell morphology and nuclear structure of *FLEH* cells after treatment with DNIC#4[$4x10^{-3}$M]: nuclei are shown in blue (Hoechst), actin structure and filaments are shown in green (FITC), objective 63x.

The actin structure appears more organized compared to cells treated with a high concentration of DNIC#4 (Figure 3).

When analyzing the same cells under high magnification 63x, it is clear that the actin structure consists of long, elongated, well-organized fibers. However, the filaments at the end of the cell still look loose and destructured. The nuclei are well-colored and round in shape (Figure 4).

3.2.Effect of DNIC#7 (potential cytostatic) on cell morphology and nuclear structure of multiple myeloma cells.

MM cells (control samples) were analyzed before treatment with DNIC#7 by confocal microscopy. The study results showed that in control samples, MM cells have a round shape, actin fibers are well stained, and the nuclei are also round (Figure 5).

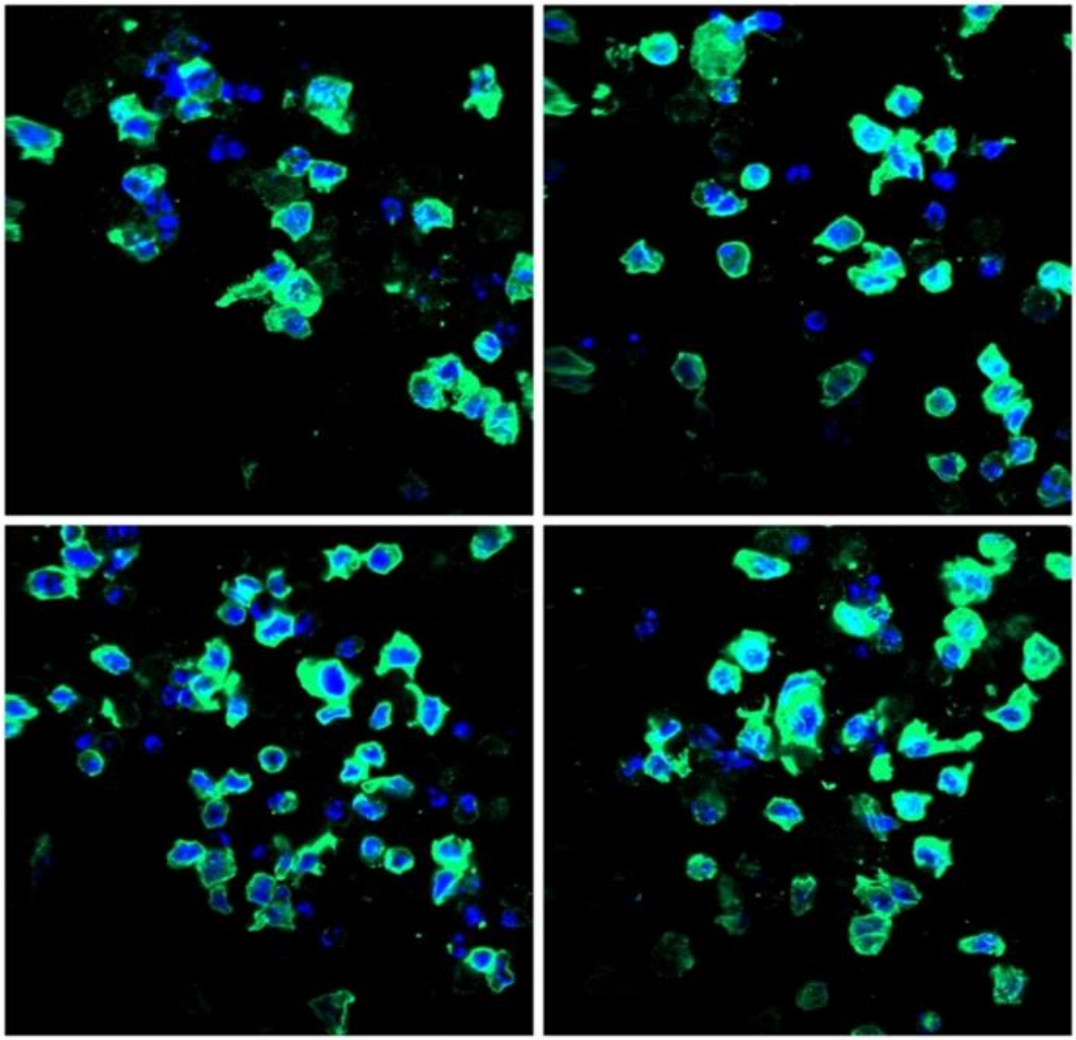

Figure 5. Confocal image of the cell morphology and nuclear structure of MM cells before treatment with DNIC#7: nuclei are shown in blue (Hoechst), while actin structure and filaments are shown in green (FITC), objective 40x. Images size – 232.5 μm x 232.5 μm.

However, after treating MM cells with DNIC#7 ($3.4x10^{-3}$M), it was difficult to determine the cell morphology. The cell structure was disrupted, damage to the cytoplasmic membrane was observed, destruction of actin fibers was observed, and only nuclei were visible, which had a fragmented shape (Figure 6).

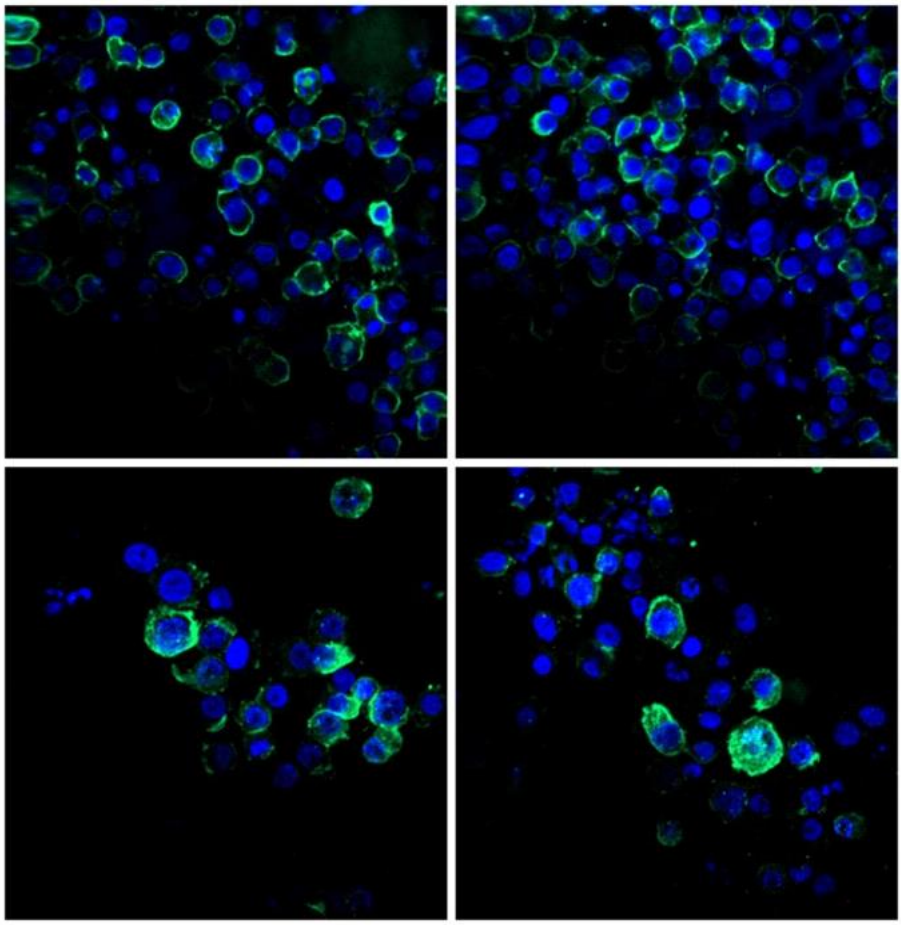

Figure 6. Cell morphology and nuclear structure of MM cells after treatment with DNIC#7[3.4x10^{-3}M]: nuclei are shown in blue (Hoechst), actin fibers are shown in green (FITC), objective 40x. Images size – 232.5 μm x 232.5 μm.

It was found that after adding DNIC#7 to the MM, the appearance of apoptotic nuclei is observed, the structure of the nuclei is destroyed, and many nuclei become fragmented (Figure 7).

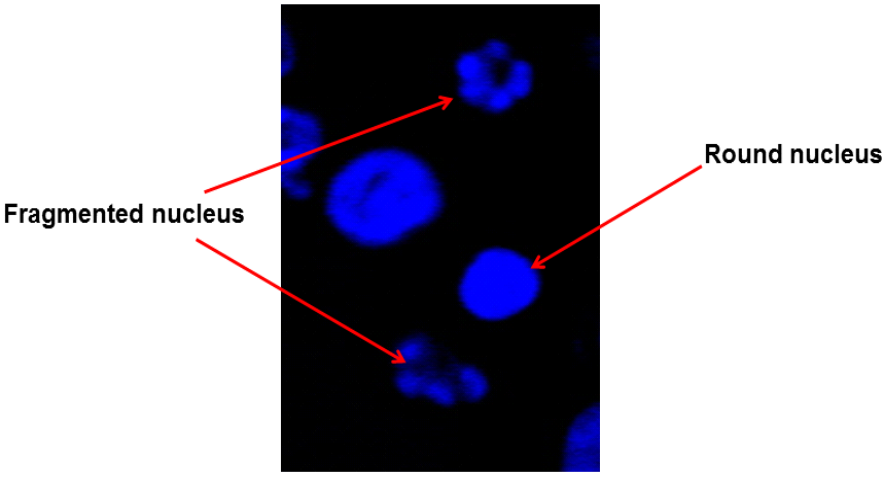

Figure 7. Confocal image of the nuclear structure of MM cells after treatment with DNIC#7[3.4x10^{-3}M]: nuclei are shown in blue (Hoechst), objective 40x.

After treating cells with DNIC#7, they found that the cell morphology changed, and the actin structure was disrupted (Figure 8).

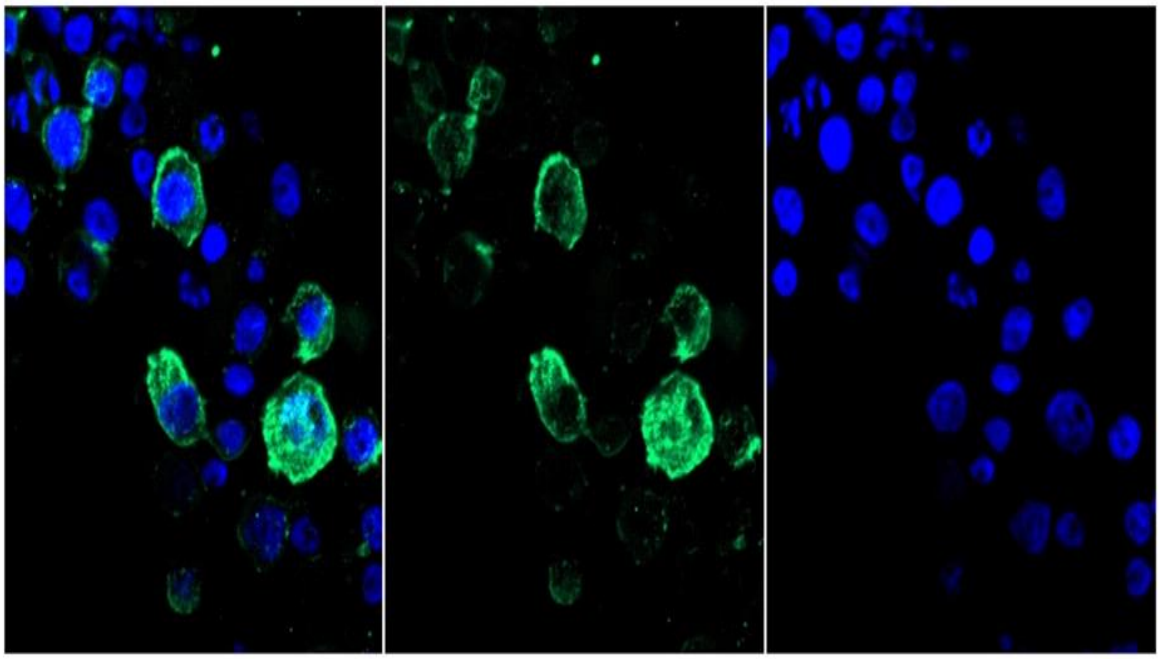

Figure 8. Cell morphology and nuclear structure of MM cells after treatment with DNIC#7[3.4x10^{-3}M]: nuclei are shown in blue (Hoechst), actin fibers are shown in green (FITC), objective 63x.

Confocal images show that as a result of exposure to DNIC#7, no staining of actin fibers is observed, the integrity of the cytoplasmic membrane is disrupted, mainly only nuclei are visible, and some of them are apoptotic and fragmented.

4. Conclusions

It is known that cell morphology is determined by a dynamic tissue matrix, which includes the extracellular matrix, cell cytoskeleton (actin fibers), nuclear matrix, and chromatin [60-64]. Mechanical and chemical signals are transmitted to the nucleus, leading to changes in the three-dimensional organization of chromatin [65-67]. Chromatin, once thought to serve only as a means to package DNA, is now recognized as a major regulator of gene activity [68, 69]. Genomic DNA in eukaryotic cells is tightly compacted with histone proteins into nucleosomes, which are further packaged into the higher-order chromatin structure. The physical structuring of chromatin is highly dynamic and regulated by a large number of epigenetic modifications in response to various environmental exposures, both in normal development and pathological processes such as aging and cancer [70, 71]. Chromatin is highly structured, and changes in its organization are essential in many cellular processes, including cell division [72, 73]. Recently, advances in machine learning have enabled researchers to automatically classify chromatin morphology in fluorescence microscopy images [74-78].

In our work, we also used the confocal fluorescence laser scanning microscopy method to analyze the cell's morphology and the nucleus's structure under the influence of DNICs to fully understand the function of DNICs in biological processes and diseases. In addition, visualization of biological structures helps to understand their function. The study results showed that when cells are treated with low concentrations of DNIC#4, slight changes in morphology, actin structure, nuclear shape, and filament structure are observed. It is likely that these changes are not dramatic for cell viability. However, when exposed to high concentrations of DNIC#4, significant changes occur in the morphology of the cell and its

shape: the cytoplasmic membrane is destroyed, the actin structure becomes diffuse, the shape of the nuclei changes, the cells “stagger”, which indicates a loss of their viability.

Thus, the results of the experiments showed that DNIC#4 at low concentrations does not exhibit cytotoxic properties and has virtually no effect on cell morphology. Our data are consistent with the results of our previous studies, in which we showed that DNIC#4 exhibits a cytoprotective effect at low concentrations [45-49].

At the same time, we have shown that DNIC#7 causes changes in the morphology of multiple myeloma cells, causing disturbances in their cytoplasmic membrane, the structure of actin fibers, and the nuclear structure. When MM cells are treated, apoptotic, highly fragmented nuclei appear. Taken together, all these changes lead to cell death, and, probably, this is due to the cytostatic effect of DNIC#7. The results of this study confirm our previous data that DNIC#7 is a cytostatic agent and has therapeutic potential for treating human multiple myeloma. [46]. We plan further studies to better understand the mechanism of action of DNIC#7 as a potential antitumor drug for treating malignant diseases.

With recent advances in confocal laser scanning microscopy, cell morphology, actin-microtubules, and nuclear structure can now be imaged with unprecedented resolution. In this work, we also used fluorescence laser scanning confocal microscopy to examine ccell morphology and nuclear structure changes under different conditions. Due to the advent of high-resolution confocal laser scanning microscopy methods, we have the opportunity to study the effect of various chemical compounds on the cytoskeleton and structure of the cell nucleus, and these methods can significantly expand our knowledge of the mechanism of action of cytoprotective or cytotoxic compounds.

Funding

The research work (synthesis of DNICs and study of their impact on cytoskeleton structure and cell morphology) was carried out with financial support within the framework of the state assignment of the Ministry of Education and Science of the Russian Federation (state registration number 124020500019-2, FFSG-2024-0012) and the Ministry of Health of the Russian Federation (project # 123021500068-8 NUYO-2023-0009 (2023-2025). Studies of the impact of DNICs on chromatin compartmentalization and nuclei morphology were performed under the state assignment of the National Research Centre "Kurchatov Institute".

Acknowledgments

The work was carried out using the equipment of the Research Center Moscow State Educational Institution “Medical Chemistry” in Chernogolovka and the equipment of the Kurchatov Genomic Center (NRC "Kurchatov Institute", Moscow). The authors would like to express their gratitude to Bespalova O.O., Shkondina N.I. and Nikishina N.S., engineers at the FRC PCP MC RAS (Chernogolovka, Moscow region, Russia), for technical assistance in preparing this publication.

Conflicts of Interest

The authors declare no conflict of interest. The funders had no role in the design of the study, in the collection, analyses, or interpretation of data, in the writing of the manuscript, or in the decision to publish the results.

References

1. Cardiovascular diseases. Available online: https://www.who.int/europe/news-room/fact-sheets/item/cardiovascular-diseases 17 July **2024**.
2. Komissarova, S.M.; Krasko, O.V.; Rineiskaya, N.M.; Sevruk, T.V.; Ustinova, I.B. Risk factors for the development of adverse cardiovascular events in patients with isolated non-compact cardiomyopathy. *Russian Cardiology Bulletin* **2022**, *17*, 67-75, https://doi.org/10.17116/Cardiobulletin20221701167.
3. Public Health. General population morbidity. Morbidity by main classes. *In Russian Statistical Yearbook Malkov P., Ed.; Stat.book/Rosstat – R76 M.: Moscow,* 30 December **2021**; p. 224. ISBN 978-5-9906962-5-9.
4. Jalepalli, S.K.; Gupta, P.; Dekker, A.L A J.; Bermejo, I.; Kar, S. Development and validation of multicentre study on novel artificial intelligence-based cardiovascular risk score (AICVD). *Fam Med Community Health* **2024**, *12*, e002340, https://doi.org/10.1136/fmch-2023-002340.
5. Kulkarni, S.; Glover, M.; Kapil, V.; Abrams, S.M.L.; Partridge, S.; McCormack, T.; Sever, P.; Delles, C.; Wilkinson, I.B. Management of hypertensive crisis: british and irish hypertension society position document. *J. Hum. Hypertens* **2023**, *37*, 863-879, https://doi.org/10.1038/s41371-022-00776-9.
6. Nazarzadeh, M.; Bidel, Z.; Canoy, D.; Copland, E.; Bennett, D.A.; Dehghan, A.; Smith, G.D.; Holman, R.R.; Woodward, M.; Gupta, A.; Adler, A.I.; Wamil, M.; Sattar, N.; Cushman, W.C.; McManus, R.J.; Teo, K.; Davis, B.R.; Chalmers, J.; Pepine, C.J.; Rahimi, K. Blood pressure lowering treatment trialists' collaboration. Blood pressure-lowering treatment for prevention of major cardiovascular diseases in people with and without type 2 diabetes: an individual participant-level data meta-analysis. *Lancet. Diabetes Endocrinol.* **2022**, *10*, 645-654, https://doi.org/10.1016/S2213-8587(22)00172-3.
7. Götzinger, F.; Kunz, M.; Lauder, L.; Böhm, M.; Mahfoud, F. Arterial hypertension-clinical trials update 2023. *Hypertens. Res.* **2023**, *46*, 2159-2167, https://doi.org/10.1038/s41440-023-01359-y.
8. Heuser, S.K.; LoBue, A.; Li, J.; Zhuge, Z.; Leo, F.; Suvorava, T.; Olsson, A.; Schneckmann, R.; Guimaraes Braga, D.D.; Srivrastava, T.; Montero, L.; Schmitz, O.J.; Schmitt, J.P.; Grandoch, M.; Weitzberg, E.; Lundberg, J.O.; Pernow, J.; Kelm, M.; Carlström, M.; Cortese-Krott, M.M. Downregulation of eNOS and preserved endothelial function in endothelial-specific arginase 1-deficient mice. *Nitric Oxide* **2022**, *125-126*, 69-77, https://doi.org/10.1016/j.niox.2022.06.004.
9. Roy, R.; Wilcox, J.; Webb, A.J.; O'Gallagher, K. Dysfunctional and dysregulated nitric oxide synthases in cardiovascular disease: mechanisms and therapeutic potential. *Int. J. Mol. Sci.* **2023**, *24*, 15200, https://doi.org/10.3390/ijms242015200.
10. Giles, A.V.; Edwards, L.; Covian, R.; Lucotte, B.M.; Balaban, R.S. Cardiac nitric oxide scavenging: role of myoglobin and mitochondria. *J. Physiol.* **2024**, *602*, 73-91, https://doi.org/10.1113/JP284446.
11. Leo, F.; Suvorava, T.; Heuser, S.K.; Li, J.; LoBue, A.; Barbarino, F.; Piragine, E.; Schneckmann, R.; Hutzler, B.; Good, M.E.; Fernandez, B.O.; Vornholz, L.; Rogers, S.; Doctor, A.; Grandoch, M.; Stegbauer, J.; Weitzberg, E.; Feelisch, M.; Lundberg, J.O.; Isakson, B.E.; Kelm, M.; Cortese-Krott, M.M. Red blood cell and endothelial eNOS independently regulate circulating nitric oxide metabolites and blood pressure. *Circulation* **2021**, *144*, 870-889, https://doi.org/10.1161/CIRCULATIONAHA.120.049606.
12. Lu, T.; Wang, Y.; Hung, C.; Chiou, S.; Liaw, W. Bioinorganic chemistry of the natural $[Fe(NO)_2]$ motif: evolution of a functional model for NO-related biomedical application and revolutionary development of a translational model. *Inorg. Chem.* **2018**, *57*, 12425-12443, https://doi.org/10.1021/acs.inorgchem.8b01818.
13. Wang ,L.; Cheng, C.K.; Yi, M.; Lui, K.O.; Huang, Y. Targeting endothelial dysfunction and inflammation. *J. Mol. Cell Cardiol.* **2022**, *168*, 58-67, https://doi.org/10.1016/j.yjmcc.2022.04.011.
14. Bryan, N.S. Nitric oxide deficiency is a primary driver of hypertension. *Biochem. Pharmacol.* **2022**, *206*, 115325, https://doi.org/10.1016/j.bcp.2022.115325.
15. Mallick, R.; Duttaroy, A.K. Modulation of endothelium function by fatty acids. *Mol Cell Biochem* **2022**, *477*, 15-38, https://doi.org/10.1007/s11010-021-04260-9.
16. DiNatale, J.C.; Crowe-White, K.M. Effects of resveratrol supplementation on nitric oxide-mediated vascular outcomes in hypertension: a systematic review. *Nitric Oxide* **2022**, *129*, 74-81, https://doi.org/10.1016/j.niox.2022.10.005.
17. He, X.; Du, T.; Long, T.; Liao, X.; Dong, Y.; Huang, Z.P. Signaling cascades in the failing heart and emerging therapeutic strategies. *Signal. Transduct. Target Ther.* **2022**, *7*, 134, https://doi.org/10.1038/s41392-022-00972-6.
18. Andreeva, V.D.; Ehlers, H.; R C AK; Presselt, M.; J van den Broek, L.; Bonnet, S. Combining nitric oxide

and calcium sensing for the detection of endothelial dysfunction. *Commun. Chem.* **2023**, *6*, 179, https://doi.org/10.1038/s42004-023-00973-8.
19. Goshi, E.; Zhou, G.; He, Q. Nitric oxide detection methods *in vitro* and *in vivo*. *Med. Gas Res.* **2019**, *9*, 192-207, https://doi.org/10.4103/2045-9912.273957.
20. Komatsu, S.; Kitazawa, T.; Ikebe, M. Visualization of stimulus-specific heterogeneous activation of individual vascular smooth muscle cells in aortic tissues. *J. Cell Physiol.* **2018**, *233*, 434-446, https://doi.org/10.1002/jcp.25903.
21. Ferrer-Sueta, G.; Campolo, N.; Trujillo, M.; Bartesaghi, S.; Carballal, S.; Romero, N.; Alvarez, B.; Radi, R. Biochemistry of peroxynitrite and protein tyrosine nitration. *Chem. Rev.* **2018**, *118*, 1338-1408, https://doi.org/10.1021/acs.chemrev.7b00568.
22. Pall, M.L. The NO/ONOO-cycle as the central cause of heart failure. *Int. J. Mol. Sci.* **2013**, *14*, 22274-22330, https://doi.org/10.3390/ijms141122274.
23. Thelitz, S.; Bekker, J.M.; Ovadia, B.; Stuart, R.B.; Johengen, M.J.; Black, S.M.; Fineman, J.R. Inhaled nitric oxide decreases pulmonary soluble guanylate cyclase protein levels in 1-month-old lambs. *J. Thorac. Cardiovasc Surg.* **2004**, *127*, 1285-1292, https://doi.org/10.1016/j.jtcvs.2003.07.024.
24. Seabra, A.B.; Duran, N. Nanoparticulated nitric oxide donors and their biomedical applications. *Mini Rev. Med. Chem.* **2017**, *17*, 216-223, https://doi.org/10.2174/1389557516666160808124624.
25. Yang, Y.; Huang, Z.; Li, L.L. Advanced nitric oxide donors: chemical structure of NO drugs, NO nanomedicines and biomedical applications. *Nanoscale* **2021**, *13*, 444-459, https://doi.org/10.1039/d0nr07484e.
26. Timoshin, A.A.; Lakomkin, V.L.; Abramov, A.A.; Ruuge, E.K.; Vanin, A.F. Hypotensive effect and accumulation of dinitrosyl iron complexes in blood and tissues after intravenous and subcutaneous injection. *Bull Exp Biol Med* **2016**, *162*, 207-210, https://doi.org/10.1007/s10517-016-3577-x.
27. Vanin, A.F. EPR Characterization of dinitrosyl iron complexes with thiol-containing ligands as an approach to their identification in biological objects: an overview. *Cell Biochem Biophys* **2018**, *76*, 3-17, https://doi.org/10.1007/s12013-017-0811-8.
28. Vanin, A.F. Positive (regulatory) and negative (cytotoxic) effects of dinitrosyl iron complexes on living organisms. *Biochemistry (Mosc)* **2022**, *87*, 1367-1386, https://doi.org/10.1134/S0006297922110153.
29. Vanin, A.F. Dinityrosyl iron complexes with thiol-containing ligands as a functionally active "working form" of nitric oxide system in living organisms: a review. *Mol. Biol. (Mosk)* **2023**, *57*, 925-937, https://doi.org/10.1134/S0026893323060183.
30. Titov, V.; Osipov, A.; Ibragimova, L.; Petrov, V.; Dolgorukova, A.; Oleshkevich, A. Hypothetical mechanism of light action on nitric oxide physiological effects. *Lasers Med. Sci.* **2021**, *36*, 1389-1395, https://doi.org/10.1007/s10103-020-03169-x.
31. Shumaev, K.B.; Gorudko, I.V.; Kosmachevskaya, O.V.; Grigorieva, D.V.; Panasenko, O.M.; Vanin, A.F.; Topunov, A.F.; Terekhova, M.S.; Sokolov, A.V.; Cherenkevich, S.N.; Ruuge, E.K. Protective effect of dinitrosyl iron complexes with glutathione in red blood cell lysis induced by hypochlorous acid. *Oxid Med. Cell Longev.* **2019**, *2019*, 2798154, https://doi.org/10.1155/2019/2798154.
32. Chen, Y.J.; Wu, S.C.; Wang, H.C.; Wu, T.H.; Yuan, S.F.; Lu, T.T.; Liaw, W.F.; Wang, Y.M. Activation of angiogenesis and wound healing in diabetic mice using NO-delivery dinitrosyl iron complexes. *Mol. Pharm.* **2019**, *16*, 4241-4251, https://doi.org/10.1021/acs.molpharmaceut.9b00586.
33. Chen, Y.C.; Chen, Y.H.; Chiu, H.; Ko, Y.H.; Wang, R.T.; Wang, W.P.; Chuang, Y.J.; Huang, C.C.; Lu, T.T. Cell-penetrating delivery of nitric oxide by biocompatible dinitrosyl iron complex and its dermato-physiological implications. *Int. J. Mol. Sci.* **2021**, *22*, 10101, https://doi.org/10.3390/ijms221810101.
34. Igrunkova, A.; Fayzullin, A.; Serejnikova, N.; Lipina, T.; Pekshev, A.; Vanin, A.; Zaborova, V.; Budanova, E.; Shestakov, D.; Kastyro, I.; Shekhter, A. Beneficial effects of dinitrosyl iron complexes on wound healing compared to commercial nitric oxide plasma generator. *Int. J. Mol. Sci.* **2023**, *24*, 4439, https://doi.org/10.3390/ijms24054439.
35. Singhal, A.; Fang, F.C. Direct and indirect inhibition of *Salmonella* peptide deformylase by nitric oxide. *MBio* **2020**, *11*, e01383-20, https://doi.org/10.1128/mBio.01383-20.
36. Wen, Z.; Zhao, Y.; Gong, Z.; Tang, Y.; Xiong, Y.; Chen, J.; Chen, C.; Zhang, Y.; Liu, S.; Zheng, J.; Li, D.; Deng, Q.; Yu, Z. The Mechanism of action of ginkgolic acid (15:1) against gram-positive bacteria involves cross talk with iron homeostasis. *Microbiol. Spectr.* **2022**, *10*, e0099121, https://doi.org/10.1128/spectrum.00991-21.
37. Sanina, N.A.; Sulimenkov, I.V.; Emel'yanova, N.S.; Konyukhova, A.S.; Stupina, T.S.; Balakina, A.A.;

Terent'ev, A.A.; Aldoshin, S.M. Cationic dinitrosyl iron complexes with thiourea exhibit selective toxicity to brain tumor cells *in vitro*. *Dalton Trans.* **2022**, *51*, 8893-8905, https://doi.org/10.1039/d2dt01011a.
38. Sahni, S.; Hickok, J.R.; Thomas, D.D. Nitric oxide reduces oxidative stress in cancer cells by forming dinitrosyliron complexes. *Nitric Oxide* **2018**, *76*, 37-44, https://doi.org/10.1016/j.niox.2018.03.003.
39. Ramírez-Patiño, R.; Avalos-Navarro, G.; Figuera, L.E.; Varela-Hernández, J.J.; Bautista-Herrera, L.A.; Muñoz-Valle, J.F.; Gallegos-Arreola, M.P. Influence of nitric oxide signaling mechanisms in cancer. *Int J Immunopathol. Pharmacol.* **2022**, *36*, 3946320221135454, https://doi.org/10.1177/03946320221135454.
40. Jibiki, I.; Hashimoto, S.; Maruoka, S.; Gon, Y.; Matsuzawa, A.; Nishitoh, H.; Ichijo, H.; Horie, T. Apoptosis signal-regulating kinase 1-mediated signaling pathway regulates nitric oxide-induced activator protein-1 activation in human bronchial epithelial cells. *Am. J. Respir. Crit. Care Med.* **2003**, *167*, 856-861, https://doi.org/10.1164/rccm.2204042.
41. Sakai, Y.; Morikawa, Y.; Nagao, Y.; Hattori, J.; Suenami, K.; Yanase, E.; Takayama, T.; Ikari, A.; Matsunaga, T. 4'-Iodo-α-pyrrolidinononanophenone provokes differentiated SH-SY5Y cell apoptosis through downregulating nitric oxide production and Bcl-2 expression. *Neurotox. Res.* **2022**, *40*, 1322-1336, https://doi.org/10.1007/s12640-022-00546-y.
42. Sanina, N. A.; Aldoshin, S. M.; Shmatko, N. Y. et al. Nitrosyl iron complexes with enhanced NO donating ability: synthesis, structure and properties of a new type of salt with the DNIC cations $[Fe(SC(NH_2)_2)_2(NO)_2]$. *New J. Chem.* **2015**, *39*, 1022-1030, https://doi.org/10.1039/C4NJ01693A.
43. Shmatko, N. Yu.; Korchagin, D. V.; Shilov, G. V.; Sanina, N. A.; Aldoshin, S. M. Molecular and crystal structure of the cationic dinitrosyl iron complex with 1,3-dimethylthiourea. *Journal of structural chemistry* **2017**, *58*, 398-400, https://doi.org/10.1134/S0022476617020172.
44. Akentieva, N.P.; Sanina, N.A.; Gizatullin, A.R.; Shmatko, N.Y.; Goryachev, N.S.; Shkondina, N.I.; Prikhodchenko, T.R.; Aldoshin, S.M. The inhibitory effect of dinitrosyl iron complexes (NO donors) on myeloperoxidase activity. *Dokl Biochem. Biophys.* **2017**, *477*, 389-393, https://doi.org/10.1134/S1607672917060126.
45. Gizatullin, A.R.; Akentieva, N.P.; Sanina, N.A.; Shmatko, N.Y.; Goryachev, N.S.; Shkondina, N.I.; Prichodchenko, T.R.; Zhelev, N.; Aldoshin, S.M. Effect of dinitrosyl iron complexes (NO donors) on the metabolic processes in human fibroblasts. *Dokl Biochem. Biophys.* **2018**, *483*, 337-340, https://doi.org/10.1134/S1607672918060133
46. Akentieva, N.P.; Sanina, N.A.; Prichodchenko, T.R.; Gizatullin, A.R.; Shkondina, N.I.; Shushanov, S.S.; Stupina, T.S.; Aldoshin, S.M. Anticancer activity of dinitrosyl iron complex (NO donor) on the multiple myeloma cells. *Dokl Biochem Biophys* **2019**, *486*, 238-242, https://doi.org/10.1134/S1607672919030190.
47. Akentieva, N.P.; Sanina, N.A.; Gizatullin, A.R.; Shkondina, N.I.; Prikhodchenko, T.R.; Shram, S.I.; Zhelev, N.; Aldoshin, S.M. Cytoprotective effects of dinitrosyl iron complexes on viability of human fibroblasts and cardiomyocytes. *Front. Pharmacol.* **2019**, *10*, 1277, https://doi.org/10.3389/fphar.2019.01277.
48. Rosenblum, S.L. Inflammation, dysregulated iron metabolism, and cardiovascular disease. *Front Aging.* **2023,** *4*, 1124178. https://doi.org/10.3389/fragi.2023.1124178
49. Akentieva, N.; Sanina, N.; Gizatullin, A.; Shushanov, S. DNIC (nitric oxide donor) suppresses the expression of matrix metalloproteinase and poly(ADP-ribose)polymerase genes in human multiple myeloma cells. *Letters in Applied NanoBioScience* **2023**, *12*, 1-20, https://doi.org/10.33263/LIANBS133.138.
50. Akentieva, N.P.; Sanina, N.A.; Gizatullin, A.R. Dinitrosyl iron complexes (nitric oxide donors) are promising drugs for the treatment of cardiovascular diseases. *UNID RAN: Moscow, Russia*, 23 December **2022**, 1-324**,** ISBN 978-5-907366-99-2.
51. Rakova, O.A.; Sanina, N.A.; Shilov, G.V.; Strelets, V.V.; Borzova, I.B.; Kulikov, A.V.; Aldoshin, S.M. $[Bu_4N]_2[Fe_2(\mu\text{-}S_2O_3)_2(NO)_4]$: Synthesis, structure, redox properties, and EPR study. *Russ. J. Coord. Chem* **2001**, *27*, 657–663, https://doi.org/10.1023/A:1017905723120.
52. Vasil'eva, S.V.; Sanina, N.A.; Moshkovskaya, E.Y.; Rudneva, T.N.; Kulikov, A.V.; Aldoshin, S.M. Formation of dinitrosyl iron complex is a necessary step in the realization of the $Na_2[Fe_2(\mu_2\text{-}S_2O_3)_2(NO)_4]\cdot 4H_2O$ genetic activity. *Dokl. Biol. Sci* **2005**, *402*, 230–232, https://doi.org/10.1007/s10630-005-0096-8.
53. Sanina, N.A.; Aldoshin, S.M.; Shmatko, N.Y.; Korchagin, D.V.; Shilov, G.V.; Ovanesyan, N.S.; Kulikov, A.V. Mesomeric tautomerism of ligand is a novel pathway for synthesis of cationic dinitrosyl iron complexes: X-ray structure and properties of nitrosyl complex with thiourea. *Inorganic Chemistry Communications* **2014**, *49*, 44–47, https://doi.org/10.1016/j.inoche.2014.09.016.
54. Shestakov, A.F.; Shul'ga, Y.M.; Emel'yanova, N.S.; Sanina, N.A.; Aldoshin, S.M. Molecular and electronic

structure and IR spectra of mononuclear dinitrosyl iron complex $Fe(SC_2H_3N_3)(SC_2H_2N_3)(NO)_2$: a theoretical study. *Russ. Chem. Bull* **2007**, *56*, 1289–1297, https://doi.org/10.1007/s11172-007-0197-7.

55. Lyssenko, K.A.; Ananyev, I.V.; Aldoshin, S.M.; Sanina, N.A. Features of chemical bonding within the $Fe(NO)_2$ fragment for crystalline bis (thiosulfate) tetra nitrosyl di-iron tetramethyl ammonium salt as an example according to high-resolution X-ray diffraction data. *Russ. Chem. Bull.* **2015**, *64*, 2351–2360, https://doi.org/10.1007/s11172-015-1163-4.
56. Aldoshin, S.M.; Morgunov, R.B.; Palii, A.V.; Shmatko, N.Y.; Sanina, N.A. Study of magnetic behavior of salts of cationic dinitrosyl iron complexes with thiocarbamide and its derivatives. *Appl. Magn. Reson* **2015**, *46*, 1383–1393, https://doi.org/10.1007/s00723-015-0689-9.
57. Sanina, N.A.; Rakova, O.A.; Aldoshin, S.M.; Shilov, G.V.; Shulga, Y.M.; Kulikov, A.V.; Ovanesyan, N.S. Structure of the neutral mononuclear dinitrosyl iron complex with 1,2,4-triazole-3-thione $[Fe(SC_2H_3N_3)(SC_2H_2N_3)(NO)_2]\cdot 0.5H_2O$. *Mendeleev Communications* **2004**, *14*, 1, 7–8, https://doi.org/10.1070/MC2004v014n01ABEH001768.
58. Aldoshin, S.M.; Sanina, N.A.; Shmatko, N.J.J.E.; Single-nuclear cationic dinitrosyl iron complexes, method for producing them, nitrogen monoxide donor. Patent No. RU 2567245C1 **2015**.
59. Gonçalves Lopes, R.C.F.; Silvestre, O.F.; Faria, A.R.; C do Vale, M.L; Marques, E.F.; Nieder, J.B. Surface charge tunable catanionic vesicles based on serine-derived surfactants as efficient nanocarriers for the delivery of the anticancer drug doxorubicin. *Nanoscale* **2019**, *11*, 5932–5941, https://doi.org/10.1039/c8nr06346j.
60. Bonifacio, M.A.; Mariggiò, M.A. New trends in pathology: from cell morphology to molecular medicine. *Int J Mol Sci*. **2023,** *24*, 11743. https://doi.org/10.3390/ijms241411743
61. Salimov, D.; Lisovskaya, T.; Otsuki, J.; Gzgzyan, A.; Bogolyubova, I.; Bogolyubov, D. Chromatin Morphology in Human Germinal Vesicle Oocytes and Their Competence to Mature in Stimulated Cycles. *Cells* **2023**, *12*, 1976, https://doi.org/10.3390/cells12151976
62. Li, Y.E.; Preissl, S.; Miller, M.; Johnson, N.D.; Wang, Z.; Jiao, H.; Zhu, C.; Wang, Z.; Xie, Y.; Poirion, O.; Kern, C.; Pinto-Duarte, A.; Tian, W.; Siletti, K.; Emerson, N.; Osteen, J.; Lucero, J.; Lin, L.; Yang, Q.; Zhu, Q.; Zemke, N.; Espinoza, S.; Yanny, A.M.; Nyhus, J.; Dee, N.; Casper, T.; Shapovalova, N.; Hirschstein, D.; Hodge, R.D.; Linnarsson, S.; Bakken, T.; Levi, B.; Keene, C.D.; Shang, J.; Lein, E.; Wang, A.; Behrens, M.M.; Ecker, J.R.; Ren, B. A comparative atlas of single-cell chromatin accessibility in the human brain. *Science* **2023**, *382*, eadf7044, https://doi.org/10.1126/science.adf7044
63. Givony,T.; Leshkowitz, D.; Del Castillo, D.; Nevo, S.; Kadouri, N.; Dassa, B.; Gruper, Y.; Khalaila, R.; Ben-Nun, O.; Gome, T.; Dobeš, J.; Ben-Dor, S.; Kedmi, M.; Keren-Shaul, H.; Heffner-Krausz, R.; Porat, Z.; Golani, O.; Addadi, Y.; Brenner, O.; Lo, D.D.; Goldfarb, Y.; Abramson, J. Thymic mimetic cells function beyond self-tolerance. *Nature* **2023**, *622*, 164-172, https://doi.org/10.1038/s41586-023-06512-8
64. Zu, S.; Li, Y.E.; Wang, K.; Armand, E.J.; Mamde, S.; Amaral, M.L.; Wang, Y.; Chu, A.; Xie, Y.; Miller, M.; Xu, J.; Wang, Z.; Zhang, K.; Jia, B.; Hou, X.; Lin, L.; Yang, Q.; Lee, S.; Li, B.; Kuan, S.; Liu, H.; Zhou, J.; Pinto-Duarte, A.; Lucero, J.; Osteen, J.; Nunn, M.; Smith, K.A.; Tasic, B.; Yao, Z.; Zeng, H.; Wang, Z.; Shang, J.; Behrens, M.M.; Ecker, J.R.; Wang, A.; Preissl, S.; Ren, B. Single-cell analysis of chromatin accessibility in the adult mouse brain. *Nature* **2023**, *624*, 378-389, https://doi.org/10.1038/s41586-023-06824-9
65. Geng, J.; Kang, Z.; Sun, Q.; Zhang, M.; Wang, P.; Li, Y.; Li, J.; Su, B.; Wei, Q. Microtubule Assists Actomyosin to Regulate Cell Nuclear Mechanics and Chromatin Accessibility. *Research (Wash D C)* **2023**, *6*, 0054, https://doi.org/10.34133/research.0054
66. González-Novo, R.; de Lope-Planelles, A.; Cruz Rodríguez, M.P.; González-Murillo, Á.; Madrazo, E.; Acitores, D.; García de Lacoba, M.; Ramírez, M.; Redondo-Muñoz, J. 3D environment controls H3K4 methylation and the mechanical response of the nucleus in acute lymphoblastic leukemia cells. *Eur. J. Cell. Biol* **2023**, *102*, 151343, https://doi.org/10.1016/j.ejcb.2023.151343
67. Sumey, J.L.; Johnston, P.C.; Harrell, A.M.; Caliari, S.R. Hydrogel mechanics regulate fibroblast DNA methylation and chromatin condensation. *Biomater. Sci* **2023**, *11*, 2886-2897, https://doi.org/10.1039/d2bm02058k
68. Even-Faitelson, L.; Hassan-Zadeh, V.; Baghestani, Z.; Bazett-Jones, D.P. Coming to terms with chromatin structure. *Chromosoma* **2016**, *125*, 95-110, https://doi.org/10.1007/s00412-015-0534-9.
69. Heo, S.J.; Thakur, S.; Chen, X.; Loebel, C.; Xia, B.; McBeath, R.; Burdick, J.A.; Shenoy, V.B.; Mauck, R.L.; Lakadamyali, M. Aberrant chromatin reorganization in cells from diseased fibrous connective tissue in

response to altered chemomechanical cues. *Nat. Biomed. Eng* **2023**, *7*, 177-191, https://doi.org/10.1038/s41551-022-00910-5
70. Xu, J.; Liu, Y. A guide to visualizing the spatial epigenome with super-resolution microscopy. *FEBS J.* **2019**, *286*, 3095-3109, https://doi.org/10.1111/febs.14938.
71. Shin, S.J.; Bayarkhangai, B.; Tsogtbaatar, K.; Yuxuan, M.; Kim, S.H.; Kim, Y.J.; Taghizadeh, A.; Kim, D.; Kim, D.H.; Lee, J.H.; Hyun, J.; Kim, H.W. Matrix-Rigidity Cooperates With Biochemical Cues in M2 Macrophage Activation Through Increased Nuclear Deformation and Chromatin Accessibility. *Adv. Sci. (Weinh)* **2025**, *12*, e2403409, https://doi.org/10.1002/advs.202403409
72. Schwartz, U.; Komatsu, T.; Huber, C.; Lagadec, F.; Baumgartl, C.; Silberhorn, E.; Nuetzel, M.; Rayne, F.; Basyuk, E.; Bertrand, E.; Rehli, M.; Wodrich, H.; Laengst, G. Changes in adenoviral chromatin organization precede early gene activation upon infection. *EMBO J* **2023**, *42*, e114162, https://doi.org/10.15252/embj.2023114162
73. Fritz, A.J.; Ghule, P.N.; Toor, R.; Dillac, L.; Perelman, J.; Boyd, J.; Lian, J.B.; Gordon, J.A.R.; Frietze, S.; Van Wijnen, A.; Stein, J.L.; Stein, G.S. Spatiotemporal Epigenetic Control of the Histone Gene Chromatin Landscape during the Cell Cycle. Crit. Rev. *Eukaryot. Gene Expr* **2023**, *33*, 85-97, https://doi.org/10.1615/CritRevEukaryotGeneExpr.2022046190
74. Xu, J.; Liu, Y. A guide to visualizing the spatial epigenome with super-resolution microscopy. *FEBS J* **2019,** *286*, 3095-3109, https://doi.org/10.1111/febs.14938
75. Smerdon, M.J.; Wyrick, J.J.; Delaney, S. A half century of exploring DNA excision repair in chromatin. *J. Biol. Chem* **2023**, *299*, 105118, https://doi.org/10.1016/j.jbc.2023.105118
76. Maldonado, R.; Längst, G. The chromatin - triple helix connection. *Biol. Chem* **2023**, *404*, 1037-1049, https://doi.org/10.1515/hsz-2023-0189
77. Ulicna, K.; Ho, L.T.L.; Soelistyo, C.J.; Day, N.J.; Lowe, A.R. Convolutional neural networks for classifying chromatin morphology in live-cell imaging. *In Chromosome Architecture: Methods and Protocols, Leake, M.C., Ed.; Springer US: New York, NY,* **2022**, *2476*, 17-30, https://doi.org/10.1007/978-1-0716-2221-6_3.
78. Mivelaz, M.; Fierz, B. Observing protein interaction dynamics to chemically defined chromatin fibers by co-localization single-molecule fluorescence microscopy. *Methods* **2020**, *184*, 112-124, https://doi.org/10.1016/j.ymeth.2020.01.018.